SCIENTIFIC REPORTS

OPEN

SUBJECT AREAS:
SOLAR CELLS
ELECTRICAL AND ELECTRONIC ENGINEERING

Received
28 November 2013

Accepted
3 March 2014

Published
18 March 2014

Correspondence and requests for materials should be addressed to B.K.M. (bkmin@kist.re.kr)

Printable, wide band-gap chalcopyrite thin films for power generating window applications

Sung Hwan Moon[1], Se Jin Park[1], Yun Jeong Hwang[1], Doh-Kwon Lee[2], Yunae Cho[3], Dong-Wook Kim[3] & Byoung Koun Min[1,4]

[1]Clean Energy Research Center, Korea Institute of Science and Technology, 39-1 Hawolgok-dong, Seongbuk-gu, Seoul, 136-791, Republic of Korea, [2]Photo-electronic Hybrids Research Center, Korea Institute of Science and Technology, 39-1 Hawolgok-dong, Seongbuk-gu, Seoul, 136-791, Republic of Korea, [3]Department of Physics, Ewha Womans University, 52, Ewhayeodae-gil, Seodaemun-gu, Seoul 120-750, Republic of Korea, [4]Green School, Korea University, Anam-dong Seongbuk-gu, Seoul 136-713, Republic of Korea.

Printable, wide band-gap chalcopyrite compound films ($CuInGaS_2$, CIGS) were synthesized on transparent conducting oxide substrates. The wide band-gap and defective nature of the films reveal semi-transparent and bifacial properties that are beneficial for power generating window applications. Importantly, solar cell devices with these films demonstrate a synergistic effect for bifacial illumination resulting in a 5.4–16.3% increase of the apparent power conversion efficiency compared to the simple sum of the efficiencies of the front and rear side illumination only. We also confirmed that this extra output power acquisition due to bifacial irradiation is apparently not influenced by the light intensity of the rear side illumination, which implies that weak light (e.g., indoor light) can be efficiently utilized to improve the overall solar cell efficiency of bifacial devices.

Synthesis of wide band-gap (>1.4 eV) chalcopyrite thin films is an important issue in the field of thin film solar cells because they are desirable in several aspects. First, a band-gap of 1.5 eV is closer to the optimum value for achieving the highest solar energy conversion efficiency in solar cells[1]. In addition, the higher voltage that can be achieved with wide band-gap materials is necessary in solar cell modules because energy loss due to series resistances can be reduced[2]. Wide band-gap thin film is also required for the top cells in a tandem solar cell. Apart from these general aspects, we may also consider their applications to power generating windows because wide band-gap material permits visible range light transmission.

There are many examples of building integrated photovoltaic (BIPV) applications where solar cells play a role in building envelope material concomitant with electric power generation[3]. Among them, however, solar cells applicable to a power generating window are very limited because they need to have transparent properties for visible regions of sunlight. Dye sensitized solar cells (DSSCs) have been considered to be the most promising candidate for power generating window applications to date due to their beneficial characteristics (e.g., semi-transparent, colorful, low cost, etc)[4,5]. However, at this moment, it is also agreed that DSSCs still suffer from serious shortcomings such as poor durability and unsafeness for their practical applications[6]. These hurdles mainly arise from use of a liquid electrolyte in solar cell devices because the liquid electrolyte used (e.g., acetonitrile with iodide ions) is volatile and toxic. Solid type solar cells (e.g., inorganic thin film solar cells), therefore, will be an attractive alternative for power generating window applications if they are transparent[7,8].

Among the inorganic thin film solar cells, chalcopyrite compound thin film solar cells in which $CuIn_xGa_{1-x}S_ySe_{2-y}$ (CIGSSe) film is used as an absorber layer have been considered the most promising thin film solar cells due to its various advantages such as high power conversion efficiency, long-term stability, etc[9,10]. In general, CIGSSe thin film solar cells have a typical device configuration of ZnO:Al/i-ZnO/CdS/CIGSSe/Mo-coated soda-lime glass[11]. In this architecture, sunlight cannot be transmitted through the solar cell device because an opaque Mo layer blocks light transmission.

To permit light transmission, CIGSSe thin film solar cells can be fabricated on transparent glass substrates (e.g., indium tin oxide (ITO) glass), resulting in bifacial solar cell configuration. Interestingly, this bifacial solar cell can also absorb light simultaneously from both the front and rear sides of such devices, thus generating electricity on both sides. To date a few studies regarding bifacial CIGSSe thin film solar cells have been reported[12,13]. However,

most of the studies have focused on small band-gap CIGSSe, through which light in visible range cannot be transmitted, and therefore, is not transparent. To our best knowledge, semi-transparent and bifacial CIGSSe thin film solar cells that can be used in a power generating window have not yet been investigated.

In order to fabricate semi-transparent, printable, bifacial CIGSSe thin film solar cells, we introduce two strategies into the CIGSSe absorber film preparation: wide band-gap material and a solution process. Wide band-gap CIGSSe absorber film can be achieved by increasing either the Ga or the S content in CIGSSe films.

In this study, we used sulfurized film ($CuInGaS_2$, CIGS), which was previously confirmed to have an optical band-gap of >1.5 eV[14]. A solution-based paste coating method was also used to make wide band-gap CIGS absorber film. Solution-based printing methods have been attracting much attention in CIGSSe thin film solar cells due to their advantages such as low processing capital costs, efficient resource material usage, high throughput, etc[15,16]. Various attempts have been made to develop highly efficient and reliable solution-processed CIGS thin film solar cells based on an Mo-coated glass substrate[17–19]. In general, solution-processed CIGS thin film has a porous nature, which has resulted in inefficient solar cell performance[20]. However, in the aspect of light transmission, the porous morphology of the film can be favourable[21]. Therefore, for the first time, the fabrication of low cost, semi-transparent, bifacial CIGS thin film solar cells is demonstrated based on sulfurized CIGS absorber film prepared by a paste-coating method on an ITO substrate. Three CIGS absorber films with different levels of thickness (400, 800, 1200 nm) were prepared to investigate the solar cell performance according to the absorber film thickness. Furthermore, to mimic a bifacial solar window operation (for the case of simultaneous irradiation by sunlight and indoor light) of solar cell devices (see the schematic in Fig. 1a), both sides of the device were illuminated by two solar simulators: the front side illumination was set at 1 Sun conditions and variable light intensity was used for the rear side illumination to imitate weaker indoor light.

Results

Fig. 1b shows a schematic of the solar cell configuration and photographs of completed solar cell devices with different CIGS absorber film thicknesses. The transparency of the device can be seen in Fig. 1b. To investigate the transmittance properties, UV-Vis spectroscopy data were obtained. There is almost no transmission of light smaller than a 600 nm wavelength irrespective of the film thickness. However, some portions of yellow to red light (600–750 nm) was transmitted through the CIGS films on ITO glass substrates, and it was more significant in the thinner absorber film (average transmittance in 600–750 nm wavelength was ~20% for the device with 400 nm CIGS film) (see Fig. 2). Meanwhile, about 200 nm thick low band-gap $CuInSe_2$ film (1.0 eV) can absorb more than 90% of the incident light in that wavelength region due to the small band gap nature[22].

In addition to a widened band gap, the porosity of the absorber film may influence the transparency at a given thickness[21]. The more porous the film, the less light it absorbs, and thus it is more transparent because less of the absorber material exists in the film. To confirm this, we prepared more porous CIGS film (por-CIGS) with almost identical film thickness (~400 nm) using different binder material (ethyl cellulose) for a paste solution[23] and compared its absorption coefficient (α) (see supporting information, Fig. S1). The por-CIGS film had a smaller absorption coefficient ($\alpha = 3.6 \times 10^4$ cm^{-1}) than the CIGS film prepared by the proposed method ($\alpha = 6.3 \times 10^4$ cm^{-1}) at $\lambda = 600$ nm. In terms of the solar window application, por-CIGS film is attractive, but there is a trade-off between transparency and power conversion efficiency due to current leakage[20]. We believe that a certain degree of the porosity of the CIGS film prepared by our solution-processed method contributes to the semi-transparency, and further control of the porosity is a promising strategy for successful use in a bifacial solar cell application.

The surface morphologies of the prepared films were slightly different depending on the film thickness (Fig. 3). The thinnest film (400 nm) had a relatively smooth surface, while some large crystallites formed on the surface as the film thickness increased.

Bifacial solar cell devices were constructed using the CIGS thin films of three different thickness based on substrate-type configuration (ZnO:Al/i-ZnO/CdS/CIGS/ITO glass). General deposition recipes were used for a CdS buffer layer (chemical bath deposition) and a ZnO window layer (sputtering deposition). Fig. 4a shows the current density-voltage (J-V) characteristics of the solar cell devices that were irradiated from the front side (ZnO face). Both open circuit voltage (V_{oc}) and short circuit current density (J_{sc}) increased as the film thickness increased (see Table 1). The highest power conversion efficiency, therefore, was obtained by the device with a 1200 nm thick CIGS film, which had the best power conversion efficiency, 5.61%. On the other hand, for the rear side illumination, different J-V behaviors were seen in which the highest efficiency was found in the device with the 800 nm thick CIGS film (1.01%) (Fig. 4a). The solar cell efficiencies of the CIGS films grown on ITO were lower than those prepared on Mo-coated soda lime glass[14]. One reason for this may be from the electrical characteristics of ITO/CIGS interface (details in Supporting Information, Fig. S2).

Notably, the efficiency gap between the front and the rear side became larger as the CIGS film thickness increased. This different behavior between the front and rear side illumination can be attributed to the large collection loss for the rear side illumination. In rear

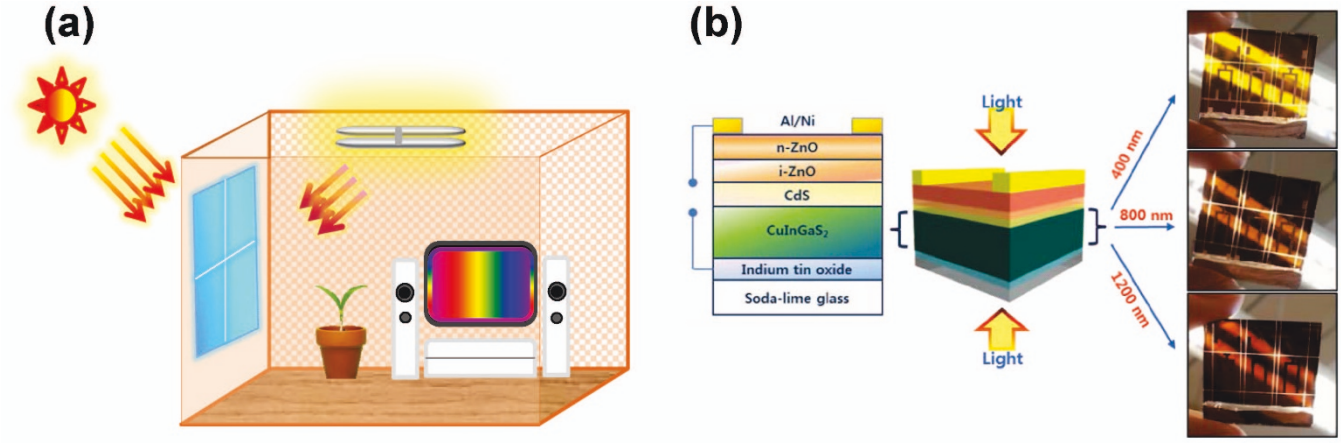

Figure 1 | (a) A schematic of power generating window applications of thin film solar cells and (b) a schematic of solar cell configuration (left) and photographs of completed solar cell devices with different CIGS absorber film thicknesses (right).

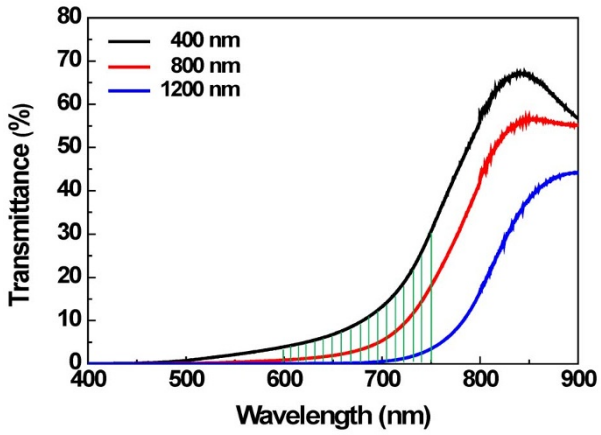

Figure 2 | **Transmittance of CIGS films with different thicknesses.**

side illumination, when the absorber layer is thick, most photons are absorbed in the region far from the space-charge region near the CdS/CIGS junction; therefore, photo-generated electrons have to travel a longer distance before they arrive at the space-charge region, which leads to a higher recombination probability. Electrons in the solution-processed CIGS absorber films have more opportunities to recombine with holes because of the poorer crystal quality (small grain size, large grain boundaries, impurities, etc.) compared to the vacuum-processed films[24].

Quantum efficiency (*QE*) is proportional to the product of the efficiencies for absorption (η_a) and collection (η_c), *i.e.*, $QE \propto \eta_a \times \eta_c$. In spite of there being less absorption loss in the thick CIGS films, the substantial decrease in J_{sc} of the thick CIGS device for the rear side illumination clearly indicates that the collection efficiency (η_c) of the devices decreases. Thus, we may presume that the diffusion length of the CIGS film prepared by the solution-coating method is not as long as the film thickness (e.g., 1200 nm). Significant collection loss ($\eta_c < 1$), hence *QE* loss for the rear side illumination, was further elucidated in the IPCE data, as can be seen in Fig. 4b.

The IPCE with front side illumination (Fig. 4b) shows an overall increase in intensity with an increasing CIGS film thickness in the entire wavelength regime. A closer look, however, reveals that the QE at wavelength below 535 nm already saturates for the device with 800 nm thick CIGS, while, at wavelength above 535 nm, increasing the thickness further up to 1200 nm. This result is explained by the fact that the penetration depth of the CIGS is longer with a longer wavelength. On the other hand, the IPCE with rear side illumination (Fig. 4b) exhibits quite different features: the highest *QE* occurs at a wavelength in a range of 700 to 800 nm depending on the CIGS thickness. Moreover, for a shorter wavelength, the *QE* drastically decreases with an increasing film thickness. Provided that the diffusion length of photo-generated electrons is less than the film thickness in CIGS, the electrons generated far from the CIGS/CdS interface cannot contribute to the photocurrent due to recombination. Therefore, the thicker the CIGS film, the lower the collection efficiency, as indicated by the decrease of *QE* in the short wavelength regime. Photons with higher penetration depth, *i.e.*, a longer wavelength may excite the electronic carriers near the CIGS/CdS interface, which can be readily collected by the electric field in the space-charge region, resulting in the highest *QE* in the longer wavelength regime.

To investigate the bifacial illumination effects on solar cell performance, light was irradiated on both sides of the device simultaneously using two standard solar simulators. Fig. 5a and Fig. S3 shows comparisons of the solar cell performance of the front side only, rear side only, and bifacial illumination with respect to the CIGS film thickness under 1 Sun conditions. The V_{oc} of the bifacial illumination is almost identical to the front illumination only for devices with 800 and 1200 nm thick films (see Supporting Information, Fig. S3). Meanwhile, substantial increases of J_{sc} were seen in the bifacial illumination for all of the devices, and these increases were much more significant for thinner absorber films (Fig. S3). Notably, the highest apparent power conversion efficiency (6.37%) was obtained by the device with the 1200 nm thick CIGS film for illumination of both sides at 1 Sun conditions (100 mW/cm^2), which value is 0.76% higher than that for the front only illumination with the same device (Fig. 5a).

To mimic the relatively weak light illumination toward the rear side by indoor light sources, we also varied the light intensity of the rear side illumination while the front side was maintained under 1 Sun conditions. The light intensities of the rear side illumination were measured with the current densities of a Si standard cell. It was obvious that the apparent power conversion efficiencies decreased as the illumination intensities of the rear side decreased (see Supporting Information, Fig. S4). We also found that the significant efficiency loss can be attributed not to the front side but to the rear side illumination, irrespective of the CIGS film thickness (Fig. S4).

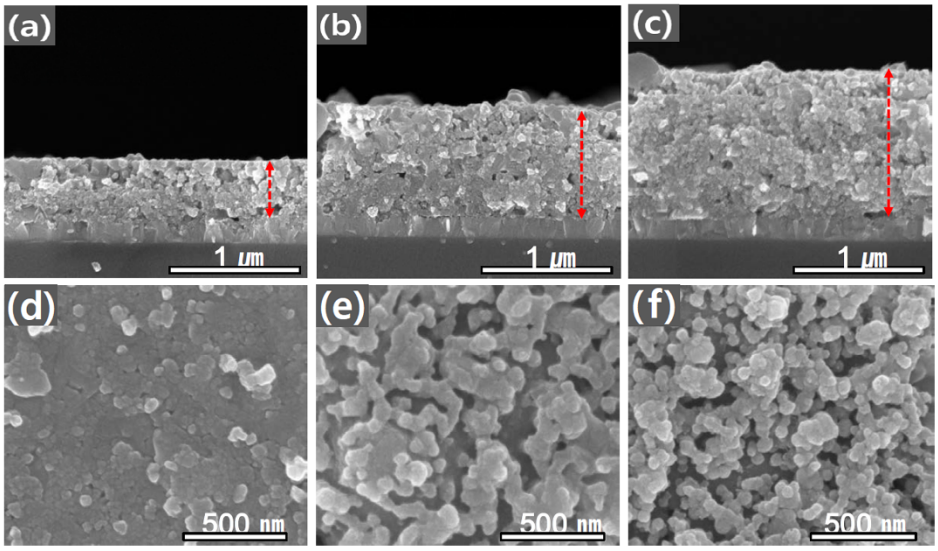

Figure 3 | Cross-sectional (a–c) and top view (d–f) SEM images of three different thick CIGS films. (a and d) 400 nm, (b and e) 800 nm, and (c and f) 1200 nm. Arrows indicate the CIGS film thickness.

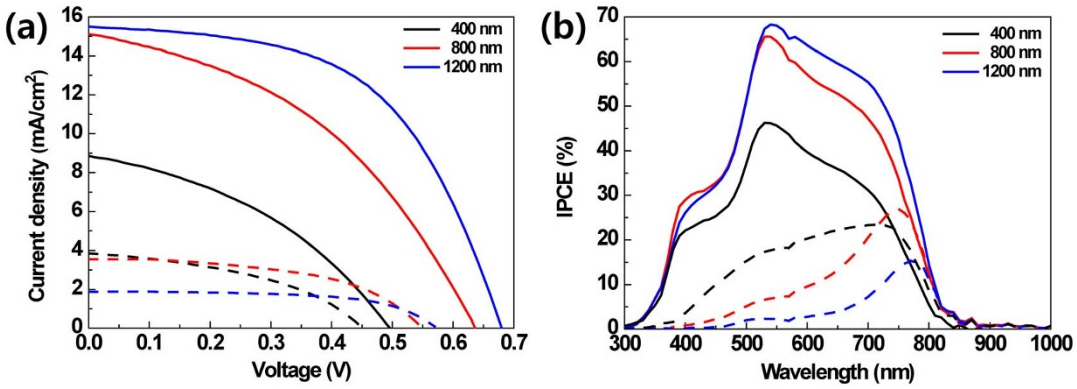

Figure 4 | (a) J-V characteristics under illumination of 1 Sun conditions and (b) IPCE spectra of CIGS solar cell devices with different levels of film thickness. (Solid lines: front side illumination; dashed lines: rear side illumination).

Interestingly, the efficiencies of bifacial illumination are slightly higher than the simple sum of only the front and rear side illumination, which suggests the presence of synergistic effects in the bifacial solar cell configuration (Fig. 5a). This efficiency enhancement is not an artifact related to both side illuminations by two solar simulators because no such enhancement was observed when solar cell devices in which the rear side was shielded by attaching an Mo-coated glass or black tape were tested under the identical irradiation conditions. In addition, the efficiency enhancement was consistently observed irrespective of the light intensity of the rear side illumination (Fig. 5b). As can be seen in Fig. 5a, the highest enhancement was observed in the device with the 800 nm thick CIGS film, while the lowest enhancement was found in the device with the 1200 nm thick CIGS film. These trends seem to be similar to those of the power conversion efficiency of the rear side illumination for the same device (Fig. 4a).

To examine the origin of the synergic effect in the bifacial solar cell configuration, the QE of the devices were measured with a background (bias) light from a white light LED with an intensity of 10 mW/cm^2 (0.1 Sun) measured by a standard Si solar cell (see Supporting Information, Fig. S5). The *QE* of the devices for front side illumination was enhanced by applying the bias light, particularly in a wavelength longer than 550 nm, and the degree of the enhancement increased with an increasing CIGS thickness. The trap sites in the CIGS film of the present study may be filled with the photoelectrons generated by the bias light, thus resulting in an increase of the collection efficiency[25]. It is also noted that the enhancement of *QE* by superimposing the bias light is indeed a unique feature of the CIGS prepared by the solution-coating method in this study. On the basis of the above discussion, we finally suggest that the synergetic efficiency gain of the bifacial solar cell may be attributed to the filling the trap sites in CIGS thin film by the rear side illumination. Under bifacial illumination, the photons incident at the rear side may act partly as a bias light near the CIGS/ITO interface and hence increase the collection efficiency for the electrons generated by the front illumination, particularly in the longer wavelength regime.

Discussion

Semi-transparent and bifacial CIGS solar cell devices were fabricated using a low cost solution-based coating method for CIGS absorber films, which can potentially be used for power generating windows. Light transmission of visible light in the CIGS film was attributed to both the film thickness and the porous nature of the film. The highest power conversion efficiency of the solar cell devices was obtained in the CIGS film with a thickness of 1200 nm when both sides of the device were illuminated with 1 Sun conditions. However, the enhancement of efficiency due to the bifacial configuration was found to be more pronounced in the device with thinner CIGS film (highest with 800 nm), showing about a 16% additional synergic efficiency increase compared to the simple efficiency sum of the front and rear side illumination only. We suggested that this extra efficiency gain is attributable to the increase of the photoexcited charge collection efficiency of the solution-processed bifacial solar cell in which rear side absorption of light plays a role as bias light filling trap sites.

Methods

A precursor mixture solution was prepared by dissolving appropriate amounts of $Cu(NO_3)_2{\cdot}xH_2O$ (99.999%, Alfa Aesar, 1.0 g), $In(NO_3)_3{\cdot}xH_2O$ (99.99%, Alfa Aesar, 1.12 g), and $Ga(NO_3)_3{\cdot}xH_2O$ (99.999%, Alfa Aesar, 0.41 g) in methanol (7.0 ml), followed by adding of a methanol solution (7.0 ml) with polyvinyl acetate (PVA, Sigma-Aldrich, 1.0 g). After the mixture solution was stirred with a magnetic bar for 30 min, a paste suitable for spin coating was prepared.

The paste was spin-casted on an ITO glass substrate (Samsung Corning, ~8 Ω/□), and the film was dried on a hotplate at 150°C for 3 min and subsequently at 250°C for 7 min. To obtain the desired thickness of the film, the above process was repeated

Table 1 | Solar cell performance results of bifacial solar cell devices with different levels of CIGS film thickness

CIGS film thickness(nm)	Illumination side	V_{oc} (V)	J_{sc} (mA/cm^2)	FF (%)	Eff. (%)
400	Bifacial	0.516	13.2	44.7	3.03[a)]
	Front only	0.495	8.86	40.8	1.70
	Rear only	0.458	3.81	42.5	0.74
800	Bifacial	0.624	19.9	43.8	5.45[a)]
	Front only	0.634	15.1	41.5	3.98
	Rear only	0.557	3.60	50.3	1.01
1200	Bifacial	0.665	17.6	53.9	6.37[a)]
	Front only	0.680	15.5	54.1	5.61
	Rear only	0.580	1.86	61.7	0.62

[a)]The efficiency values of bifacial illumination are apparent solar energy conversion efficiencies (not real efficiencies) obtained by assuming light irradiation under 1 Sun condition even though both sides of the solar cells were illuminated simultaneously.

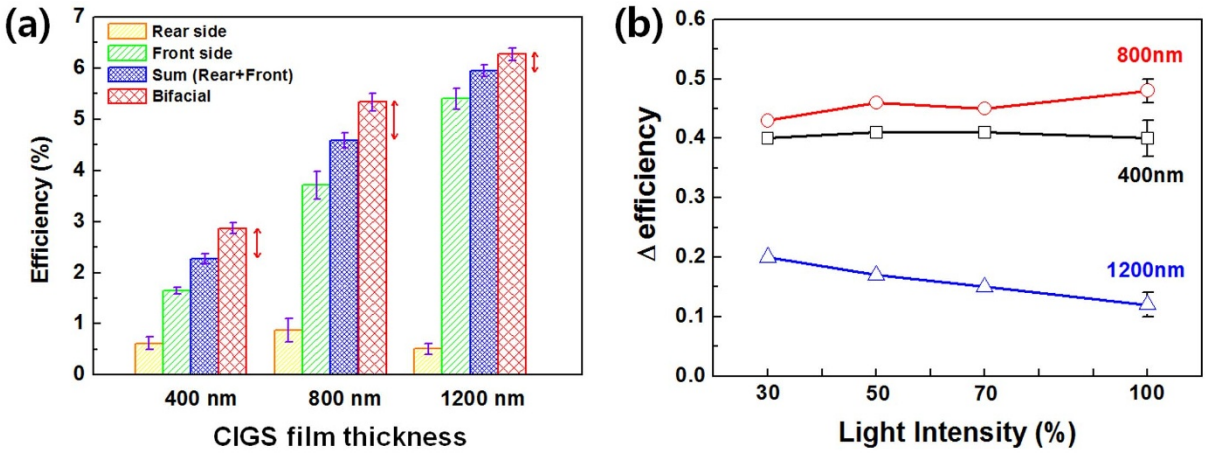

Figure 5 | (a) Solar cell efficiencies of the devices with different levels of CIGS film thickness for front and rear side illumination only, numerical sum of front and rear side illumination only, and bifacial illumination under 1 Sun conditions. Arrows indicate the extra increase in efficiency due to bifacial illumination. The efficiencies are average values of ten solar cell devices with different levels of CIGS film thickness. (b) Extra gains of solar cell efficiencies due to bifacial illumination with respect to irradiated light intensities toward the rear side. Light intensity in X-axis is presented by the percentage of J_{sc} with respect to that of 1 Sun irradiation, which was measured by a standard Si solar cell.

(generally ~200 nm thick film was obtained for each deposition). After coating and drying, the first annealing process, air annealing, was performed at 300°C for 30 min under ambient conditions. The second annealing process, sulfurization, was carried out at 500°C for 30 min under $H_2S(1\%)/N_2$ gas environment.

A solar cell device was fabricated according to a substrate-type configuration (ZnO:Al/i-ZnO/CdS/CIGS/ITO glass). A 60 nm-thick CdS buffer layer was prepared on the CIGS film by chemical bath deposition (CBD), and i-ZnO (50 nm)/Al-doped n-ZnO (500 nm) was deposited by the radio frequency magnetron sputtering method. A Ni/Al (50/500 nm) grid was prepared as a current collector by thermal evaporation. The active area of the completed cell was 0.44 cm^2.

Structural characterization of the films was performed using a scanning electron microscope (SEM, FEI, Nova-Nano200) with a 10 kV acceleration voltage and an X-ray diffractometer (XRD, Shimadzu, XRD-6000) with Cu-Kα radiation (λ = 0.15406 nm). The film thickness was measured with a surface profiler (Veeco, Dektak 8). Optical properties of the CIGS films were measured by a UV-Vis spectrometer (Varian, Cary 5000). Device performances were characterized using a solar simulator (ABET Technologies, Inc., Sun 2000) and an incident photon-to-current conversion efficiency (IPCE) measurement unit (PV measurement Inc.). During the IPCE measurement, background light (LED, Daejin DMP Co.) was applied in some cases.

To investigate the interfacial properties between CIGS and ITO layers, temperature dependent dark current density-voltage measurement was also carried out using a Keithley 4200 semiconductor characterization system and a cryogenic vacuum probe station (ST-500, Janis Co.).

1. Green, M. SOLAR CELLS: Operating Principles, Technology and System Applications. *Prentice-Hall* New Jersey, USA, (1982).
2. Siebentritt, S. Wide gap chalcopyrites: material properties and solar cells. *Thin Solid Films* **403–404**, 1–8 (2002).
3. Benemann, J., Chehab, O. & Schaar-Gabriel, E. Building-integrated PV modules. *Sol. Energy Mater. Sol. Cells* **67**, 345–354 (2001).
4. Goncalves, L. M., Bermudez, V. D., Ribeiro, H. A. & Mendes, A. M. Dye-sensitized solar cells: A safe bet for the future. *Energy Environ. Sci.* **1**, 655–667 (2008).
5. Yoon, S. *et al.* Application of transparent dye-sensitized solar cells to building integrated photovoltaic systems. *Build. Environ.* **46**, 1899–1904 (2011).
6. Hinsch, A. *et al.* Long-term stability of dye-sensitised solar cells. *Prog. Photovolt.: Res. Appl.* **9**, 425–438 (2001).
7. Ng, P. K., Mithraratne, N. & Wittkope, S. Semi-Transparent Building-Integrated Photovoltaic Windows: Potential Energy Saving of Office Buildings in Tropical Singapore. *PLEA2012 28th Conference: Opportunities, Limits & Needs Towards an environmentally responsible architecture,* Lima Peru, (2012, Nov, 7–9).
8. Yoon, J. H., Song, J. & Lee, S. J. Practical application of building integrated photovoltaic (BIPV) system using transparent amorphous silicon thin-film PV module. *Sol. Energy* **85**, 723–733 (2011).
9. Hegedus, S. Thin film solar modules: The low cost, high throughput and versatile alternative to Si wafers. *Prog. Photovolt.: Res. Appl.* **14**, 393–411 (2006).
10. Green, M. A., Emery, K., Hishikawa, Y., Warta, W. & Dunlop, E. D. Solar cell efficiency tables (version 40). *Prog. Photovolt.: Res. Appl.* **20**, 606–614 (2012).
11. Kemell, M., Ritala, M. & Leskela, M. Thin film deposition methods for $CuInSe_2$ solar cells. *Crit. Rev. Solid State Mater. Sci.* **30**, 1–31 (2005).
12. Young, D. L. *et al.* A new thin-film $CuGaSe_2/Cu(In,Ga)Se_2$ bifacial, tandem solar cell with both junctions formed simultaneously. *Proceeding of the 29th IEEE PVSC,* New Orleans USA, 608–611 (2002, May, 20–24).
13. Nakada, T. *et al.* Bifacial CIGS thin film solar cells. *20th European Photovoltaic Solar Energy Conference,* Barcelona Spain, 1736–1739 (2005, June, 6–10).
14. Park, S. J. *et al.* Solution processed high band-gap $CuInGaS_2$ thin film for solar cell applications. *Prog. Photovolt.: Res. Appl.* **22**, 122–128 (2014).
15. Hibberd, C. J. *et al.* Non-vacuum methods for formation of $Cu(In,Ga)(Se,S)_2$ thin film photovoltaic absorbers. *Prog. Photovolt.: Res. Appl.* **18**, 434–452 (2010).
16. Habas, S. E., Platt, H. A. S., van Hest, M. F. A. M. & Ginley, D. S. Low-Cost Inorganic Solar Cells: From Ink To Printed Device. *Chem. Rev.* **110**, 6571–6594 (2010).
17. Todorov, T. K., Gunawan, O., Gokmen, T. & Mitzi, D. B. Solution-processed $Cu(In,Ga)(S,Se)_2$ absorber yielding a 15.2% efficient solar cell. *Prog. Photovolt.: Res. Appl.* **21**, 82–87 (2012).
18. Guo, Q., Ford, G. M., Agrawal, R. & Hillhouse, H. W. Ink formulation and low-temperature incorporation of sodium to yield 12% efficient $Cu(In,Ga)(S,Se)_2$ solar cells from sulfide nanocrystal inks. *Prog. Photovolt.: Res. Appl.* **21**, 64–71 (2012).
19. Jeong, S. *et al.* An 8.2% efficient solution-processed $CuInSe_2$ solar cell based on multiphase $CuInSe_2$ nanoparticles. *Energy Environ. Sci.* **5**, 7539–7542 (2012).
20. Uhl, A. R., Romanyuk, Y. E. & Tiwari, A. N. Thin film $Cu(In,Ga)Se_2$ solar cells processed from solution pastes with polymethyl methacrylate binder. *Thin Solid Films* **519**, 7259–7263 (2011).
21. Ding, S. J. *et al.* Tunable Assembly of Vanadium Dioxide Nanoparticles to Create Porous Film for Energy-Saving Applications. *Acs Appl. Mater. Inter.* **5**, 1630–1635 (2013).
22. Jaffe, J. E. & Zunger, A. Theory of the Band-Gap Anomaly in Abc_2 Chalcopyrite Semiconductors. *Phys. Rev. B.* **29**, 1882–1906 (1984).
23. Lee, E. *et al.* Nearly carbon-free printable CIGS thin films for solar cell applications. *Sol. Energy Mater. Sol. Cells* **95**, 2928–2932 (2011).
24. Akhavan, V. A. *et al.* Spray-deposited $CuInSe_2$ nanocrystal photovoltaics. *Energy Environ. Sci.* **3**, 1600–1606 (2010).
25. van de Lagemaat, J., Park, N. G. & Frank, A. J. Influence of Electrical Potential Distribution, Charge Transport, and Recombination on the Photopotential and Photocurrent Conversion Efficiency of Dye-Sensitized Nanocrystalline TiO_2 Solar Cells: A Study by Electrical Impedance and Optical Modulation Techniques. *J. Phys. Chem. B.* **104**, 2044–2052 (2000).

Acknowledgments

This work was supported by a National Research Foundation of Korea Grant (NRF-2009-C1AAA001-0092935 and University-Institute cooperation program) and partly by the "National Agenda Project" program of the Korea Research Council of Fundamental Science & Technology (KRCF), funded by the Ministry of Science, ICT and Future Planning. Also, the authors would like to thank the program of the Korea Institute of Science and Technology (KIST).

Author contributions

B.K.M. planned the project. S.H.M. and S.J.P. managed and performed all the detailed experiment, and Y.C., D.L., Y.J.H. and D.K. helped data analysis and manuscript preparation. All the authors discussed the results and commented on the manuscript.

Additional information

Supplementary information accompanies this paper at http://www.nature.com/scientificreports

Competing financial interests: The authors declare no competing financial interests.

How to cite this article: Moon, S.H. *et al.* Printable, wide band-gap chalcopyrite thin films for power generating window applications. *Sci. Rep.* **4**, 4408; DOI:10.1038/srep04408 (2014).